33rd Annual International Conference of the IEEE EMBS
Boston, Massachusetts USA, August 30 - September 3, 2011

# The Electric Field System of a Macular Ion Channel Plaque

Colin G. Hales, *Student Member, IEEE*., David B. Grayden, and Harry Quiney

***Abstract*—Recent empirical neuroscience evidence increasingly supports an active role for the endogenous electromagnetic (EM) field system of brain tissue. These results undermine the long-held view that the field system is a causally inert byproduct of action potential and synapse electrochemical activity. The dominant originating mechanism for the endogenous EM field remains undetermined. The new observations make the isolation of an unambiguous original EM field source a matter of some urgency. As part of the process of elaboration of the field systems produced by coherent transmembrane filamentary currents (the most plausible original mechanism), this paper looks at the contribution by a localized density of cooperating ion channels in the form of the macular synaptic plaque engaged in conducting a post-synaptic current. The method uses the volume conduction formalism driven by filamentary currents that stand in for ion channels. Not surprisingly, the result is a pulsing dipole. Despite its extreme material abstraction, the result forms one of the basic mechanisms for future models capable of revealing whole-neuron and network-level endogenous EM field system.**

## I. Introduction

THE endogenous electromagnetic field in nervous tissue is in the midst of a significant change in status. Recent empirical results increasingly indicate that the electromagnetic field is actively involved in the kindling/modulation of dynamics from the sub-neuron level to the whole tissue. This undermines the long-held view that the EM fields are a functionally inert epiphenomenon of synapse/action potential (neuronal network) activity. It is becoming clear that, despite their small magnitude, their impact is magnified through the action potential phase sensitivity around the critical threshold of firing. Sustained microscopic endogenous EM effects then lead to tissue entrainment at ever greater scales. The medical term that refers to the active EM coupling of tissue regions is called ephapsis [1-3].

The endogenous EM field is originated microscopically by ion activity and, in its microscopic domain, it tends to be called the extracellular field. The acronym LFP stands for local field potential (a scalar potential), is measured by an invasive probe, and reveals the electric field. At increasing spatial scales, the superposing EM fields from myriad neurons accretes, inheriting the microscopic organizational structure of the host tissue. In the case of brain tissue, eventually the fields emerge at the brain surface and, ultimately, the scalp, where the electric field is revealed by an average voltage measurement named 'field potential'. In this context, the electric field is witnessed in the EEG (electroencephalogram) signal. Likewise, the magnetic field is witnessed directly in the MEG (magnetoencephalogram).

Practitioners will usually say the EEG is due to synaptic activity [4, p20]. EEG can be found attributed to, at various times, 'summated action potential', 'dendritic potential', 'oscillating dipoles' and 'excitatory post-synaptic potentials' [5]. The literature generally reflects an understanding that EEG originates in the deep microscopic cortical LFP. However, the dominant specific microscopic phenomenon driving the LFP remains undetermined. Indeed, in 2009, the LFP was declared to have 'mysterious origins' [6]. The ultimate origin of the EEG is therefore a mystery older than neuroscience. With empirical results highlighting the EM field as causal, the lack of a definite mechanism behind field expression becomes a hypercritical issue.

Guided by this motivation, this paper is part of a program aimed at isolating the detail of the mechanism responsible for the LFP in a way that explains both the EEG and MEG. The straightforward way to a plausible dominant original cause of the field system is to focus on *current coherence*. It is easy to see that if coherence is the dominant determinant, then the primary originating currents for all extra-neuronal EM phenomena are the transmembrane currents. Primary transmembrane currents create a secondary intracellular space (ICS/cytosol) and extracellular space (ECS) currents. These currents are supplied by and terminate in a vast collection of paramembrane hydrated ion populations. As such, charge ECS/ICS current activity is better visualized as two large shallow pools of ions connected via ion channels. The idea is that a field system is established by the transmembrane currents, disturbing the huge transmembrane resting electric field which is of the order $10^6$ V/m to $10^7$ V/m [7, 8]. This background/resting field does not explicitly appear in the simulation model used below. The field system to be revealed is therefore only the dynamic component of the overall field system.

To understand how transmembrane current coherence dominates the field system, note that the resultant ECS and ICS currents are expressed as randomized (compared with

Manuscript received 19 Jun 2011.

C. G. Hales. NICTA VRL, Department of Electrical and Electronic Engineering, University of Melbourne, Victoria, 3010 Australia. Corresponding author. Phone: (03) 8344 4489 (International +61 3 8344 4489) Fax (03) 9348 1682 (or International +61 3 9348 1682). Email: chales@ee.unimelb.edu.au. Corresponding author.

A/Prof. D. B. Grayden. Department of Electrical and Electronic Engineering, University of Melbourne, Victoria 3010, Australia.

A/Prof H. Quiney. ARC Centre of Excellence for Coherent X-ray Science, School of Physics, University of Melbourne, Victoria 3010, Australia

the transmembrane current) charge motions. In this form the ECS/ICS current is spatially and temporally decohered at an atomic/molecular level. This contrasts with the transmembrane portion of a charge's trajectory, which is both highly spatially localized (ion channel pore) and temporally localized within the membrane-longitudinal action potential propagation path. Transmembrane ion traffic also has de-hydrated ion transit dynamics that are more localized than that of the surrounding ions and their medium [9].

In this paper, the field system produced by a planar/macular filament plaque is investigated. The plaque is an aggregate of ion channels such as that found embedded in the post-synaptic lipid bilayer of a macular chemical synapse. The actual number of ion channels, their type and their collocation preferences are not known in detail. However, basic synaptic ion channel permeability kinetics is known well enough to have a useful analytic form for the transmembrane current. This is all that is needed here.

## II. Method

### A. Volume Conduction

The most widespread an well known formalism for expressing the LFP in nervous tissue is the 'volume conduction' equation. It presupposes that Ohm's law applies and in its simplest form it produces the local field potential, at position **r** and time *t*, for an infinite uniform conductivity $\sigma$ (S/m),

$$\varphi_{LFP}(\mathbf{r},t) = \frac{1}{4\pi\sigma}\int_V \frac{I_v(\mathbf{r}',t)}{|\mathbf{r}-\mathbf{r}'|} d^3r', \tag{2}$$

where

$$I_v(\mathbf{r},t) = -\nabla \bullet \mathbf{J}_s(\mathbf{r},t) \tag{3}$$

is a volume current source density (in $A \cdot m^{-3}$) that distributes current over integration volume *V*.

A preliminary exploration of equation (2), under a '*transmembrane currents originate the LFP*' proposition, has already been conducted. It uses the transmembrane currents in equation (2) and ignores the ICS and ECS currents under the assumption that they contribute only field noise. It used the transmembrane current produced by a large compartmental cable-equation model of a single neuron (rat hippocampus CA1 pyramidal). High performance computing (HPC) enabled biological realism. So far, only an exemplar field system has been computed (i) for a single neuron, and (ii) *only for the action potential ion channel contribution*. Despite the extreme nature of the material abstraction of (2), it revealed a faint but spatially large, unified (rotating) dipole system. It also showed that the detailed field system created by coherent transmembrane current activity will depend on cell morphology and the specific expression of ion channels (type, density, collocation) throughout the neural soma and its processes, including synapses [10]. However, the contribution by synapses has not been established. It suffices to say that the magnitude of the field system produced by the model is consistent with the levels needed for the required active, independent field role in a fully elaborated tissue model.

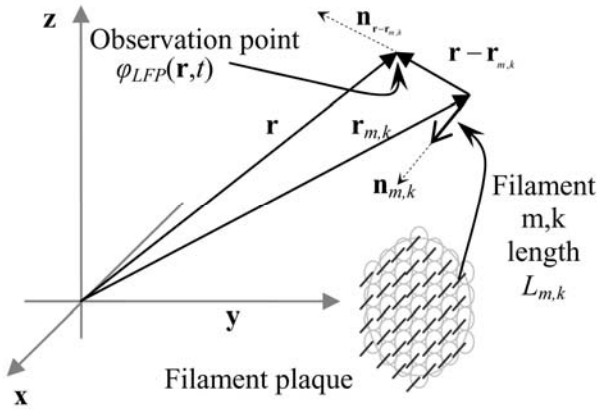


Fig. 1. The operation of equation (4) applied to a filament plaque. In this case the number of 'compartments' M = 1 and the number of filaments $K_m$ = 37.

To extend the research, a single (chemical) chemical synapse plaque contribution is to be explored. This will facilitate later investigations of more complex neural models with cohorts of realistically placed chemical synapses, each with its own post-synaptic current, realistically temporally related to the triggering of the action potential. Only then can the complete field system produced by a single neuron be computed.

### B. The Volume Conduction Model with Filament Sources

Consider a collection of *M* current filament cohorts, where cohort *m* ($1 \le m \le M$) is of size $K_m$, and where compartment *m* filament *k* carries current $i_{m,k}(t)$. Each filament is of length $L_{m,k}$, located at a position $\mathbf{r}_{m,k}$, and oriented in direction $\mathbf{n}_{m,k}$. The entire system of *M* cohorts is embedded in an infinite uniform conductivity $\sigma$. It is relatively straightforward to show that for this circumstance, (2) becomes

$$\varphi_{LFP}(\mathbf{r},t) = \frac{-1}{4\pi\sigma}\sum_{m=1}^{M}\sum_{k=1}^{K_m}\left[\frac{L_{m,k}i_{m,k}(t)\left(\mathbf{n}_{m,k}\bullet\mathbf{n}_{m,r-r_{m,k}}\right)}{|\mathbf{r}-\mathbf{r}_{m,k}|^2}\right] \tag{4}$$

for positions **r** large compared to $L_{m,k}$.[10]. See Fig 1 for basic terminology. For quasi static conditions,

$$\mathbf{E}(\mathbf{r},t) = -\nabla\varphi_{LFP}(\mathbf{r},t). \tag{5}$$

Applied to (4), (5) gives

$$\mathbf{E}(\mathbf{r},t) = \frac{1}{2\pi\sigma}\sum_{m=1}^{M}\sum_{k=1}^{K_m}\left[\frac{L_{m,k}i_{m,k}(t)\left(\mathbf{n}_{m,k}\bullet\mathbf{n}_{m,r-r_{m,k}}\right)}{|\mathbf{r}-\mathbf{r}_{m,k}|^3}\mathbf{n}_{m,r-r_{m,k}}\right]. \tag{6}$$

In practice, the total cohort current (all $K_m$ filament currents) is numerically equal to the total 'compartment' transmembrane current, where a filament 'cohort' refers to all filaments attached to a compartment. For the simulations to follow, $L_{m,k}$ = 7.5 nm is used for a typical membrane-

bilayer-spanning protein pore. The conductivity was set at $\sigma$ = 1/3 $Sm^{-1}$ [11].

In the use of (4) so far, where transmembrane compartment current is known from a cable equation action potential simulation, (i) no attempt has been made to decompose the current into particular types (e.g. capacitative vs. gated channel vs. passive) or ion channel type (e.g. $Na^+$, $K^+$ etc), and (ii) the filaments notionally stand in for pseudo-ion channels located on the compartment surface and (iii) the total transmembrane current was divided equally amongst the filaments. Here, in a chemical synapse, where we have ligand-gated ion channels, again no attempt has been made to segregate ion channel types. The simulation proceeds on a total-current basis.

### C. Post-synaptic current behaviour

$$i_{total}(t) = i_{\max}\left[e^{-(t-t_0)/\tau_1} - e^{-(t-t_0)/\tau_2}\right] \qquad (7)$$

For the purposes here, a typical total post-synaptic current can be considered to have an 'alpha-synaptic' time course as per (7), where $i_{max}$ = 60 nA, $\tau_1$ = 5.26 ms, $\tau_2$ = 0.19 ms, $t_0$ = 10.0ms [12, p181]. This current profile is shown in Fig 2. The onset delay maintains consistency with the triggering of the action potential in the original simulation. This current is divided equally between the plaque filaments.

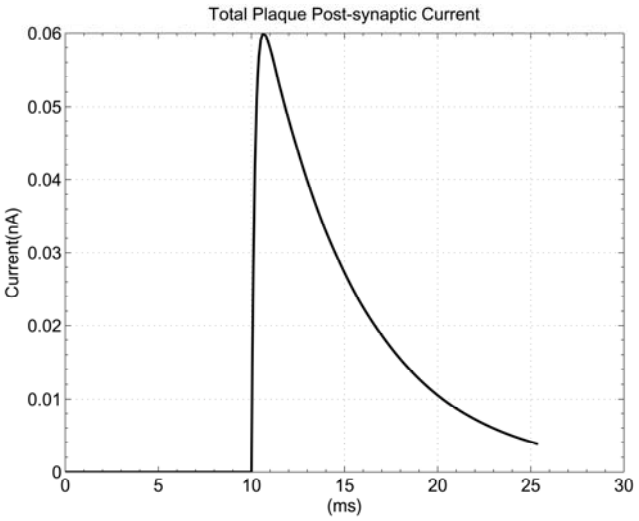


Fig. 2. The post synaptic current input to equation (4). The current is divided equally amongst all filaments. The convention is that positive current flows out of a cell. Therefore this current is functionally inhibitory (hyperpolarizing).

### D. The chemical synaptic plaque

Translating a current such as (7) into a physically realistic set of current filaments requires a bit of anatomy. The surface area of a synapse is the main issue. To establish a rough synaptic 'plaque' current filament configuration we can use [13], where we find that the synaptic volume for macular synapses ranges from $0.15x10^{-3}\mu m^3$ to $2.1x10^{-3}\mu m^3$. Given the typical synaptic cleft gap is roughly 20 nm [9, p301],[14],[15],[16], if the cleft volume is treated as a

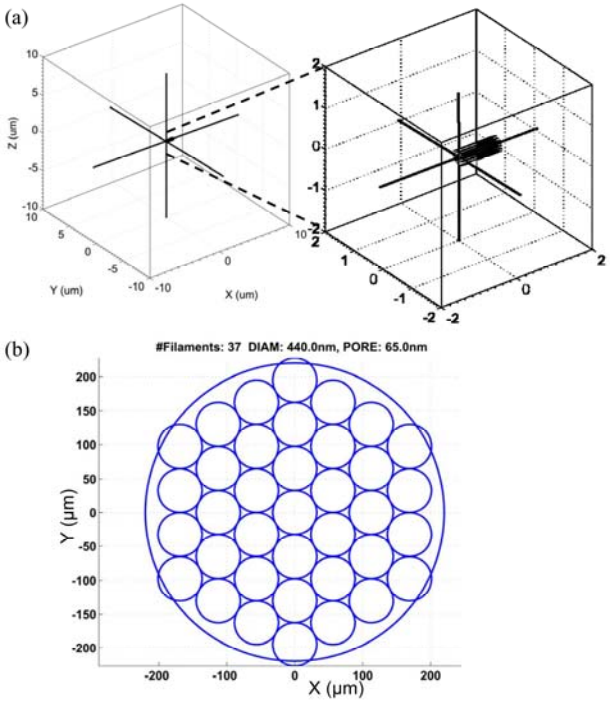


Fig. 3.The filament plaque layout (a pore at the center of each circle). The filament length is exaggerated. The plaque is located centred on the origin in the YZ plane, with the filaments pointing in the +X direction.

circular disk 20 nm high, then this suggests the post-synaptic surface area is a circle (macula) of radius between 49 nm and 183 nm. This is somewhat smaller then the radius of the active area used by [16] of ~300 nm. For the purposes here, a value of 220 nm was chosen as the radius of the plaque.

Filament distribution over the plaque surface can be established by considering that given that a typical single ion channel passes a few pA when open [9] [12], a spread of roughly 30 filaments over the synaptic plaque seems reasonable. In reality, the plaque is so small compared to the mm-scale geometry of the whole field, in practice a single filament would be adequate. However, for the sake of future simulations of tight neighborhoods of hundreds of millions of competing synaptic plaques with variable geometry, the filaments were chosen so that ion channel pores are 65 nm apart in a hexagonal close packed array. The resultant plaque and its position are shown in Fig 3. Because there is only one synapse, M = 1 in (4). Because there are 37 filaments in the plaque, $K_m = K_1 = 37$ in (4).

## III. Results

The simulation computes the LFP at times (7.802 ms $\leq t \leq$ 20.888 ms) at a spatial resolution of 1 µm. The results form a supplementary video. A faint pulsing dipole is the quite predictable result. A modified single video frame is included in Fig 4. It shows both the LFP and the electric field near the peak of the waveform (t = 10.944ms). It is interesting to note that the field system preserves a region of zero field and zero LFP along the plane that would be occupied by the membrane in the real tissue. The field system is therefore

naturally compatible with the existence of a membrane. The lower panels in Fig 4. show that the LFP at any point inherits the temporal behaviour of the filamentary source. This is to be expected from equations (4) and (6).

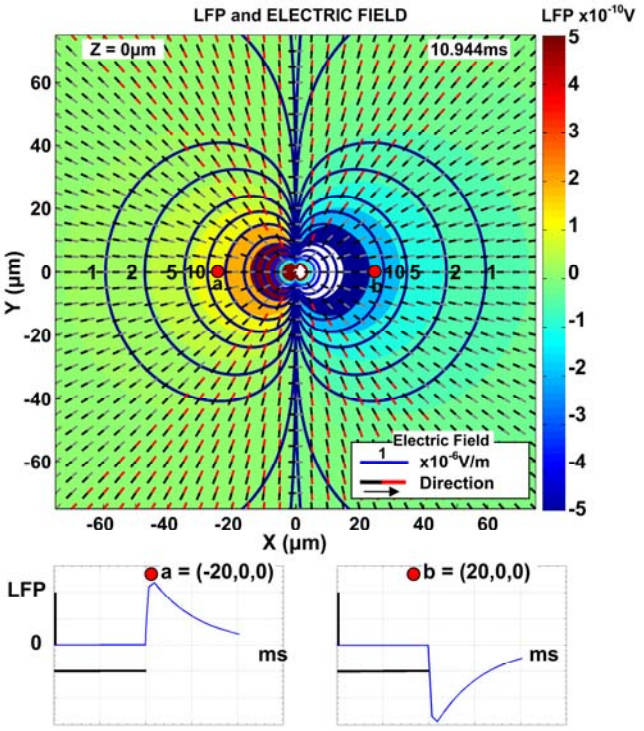


Fig. 4. TOP: XY plane snapshot at t = 10.944 ms, Z = 0. of electric field lines and iso-electric field contours. These are superimposed on the LFP. Isopotential contours match the dipolar shape of the electric field contours. Electric field vectors are two-coloured to give direction. BOTTOM: Time course at particular points a(-20,0,0) and b(20,0,0). Vertical scale bar $2x10^{-10}$V. Horizontal scale bar 10ms.

The electric field is the *gradient* of the LFP and only needs to reach 1V/m to be physiologically active [2]. In a volume of 1 $mm^3$ there are 40,000-50,000 neurons and more than $10^8$ synapses. It is their collective action that is modulated by the endogenous EM field. The depicted field system is therefore a tiny part of an extremely complex aggregate field system with a functionally significant intensity. Based on the wide spatial pattern, which exists over tens of μm, the endogenous field system can be seen to have two kinds of ephaptic influence. Physically, the electric and magnetic fields influence tissue behaviour by virtue of the Lorentz force. First, the field produced by a neuron influences itself (auto-ephapsis). Second, the same field produced by a neuron can influence other neurons (allo-ephapsis). None of these influences are found in any existing neural modelling.

Future models incorporating filament plaques and action potentials in realistic numbers will be needed to predict the electric and magnetic field found in real tissue. To elaborate the fields in biologically realistic ways, it turns out that high performance computing is the necessary tool.

## ACKNOWLEDGMENT

This research was supported by a Victorian Life Sciences Computation Initiative (VLSCI) grant number VR0003 on its Peak Computing Facility at the University of Melbourne, an initiative of the Victorian Government. NICTA is funded by the Australian Government as represented by the Department of Broadband, Communications and the Digital Economy and the Australian Research Council through the ICT Centre of Excellence program.

## REFERENCES

[1] T. Radman, et al., "Spike timing amplifies the effect of electric fields on neurons: Implications for endogenous field effects," Journal of Neuroscience, vol. 27, pp. 3030-3036, Mar 2007.

[2] C. A. Anastassiou, et al., "Ephaptic coupling of cortical neurons," Nature Neuroscience, vol. 14, pp. 217-223, 2011.

[3] F. Frohlich and D. A. McCormick, "Endogenous Electric Fields May Guide Neocortical Network Activity," Neuron, vol. 67, pp. 129-143, Jul 2010.

[4] E.-J. Speckmann and C. E. Elgar, "Introduction to the Neurophysiological Basis of the EEG and DC Potentials," in Electroencephalography : basic principles, clinical applications, and related fields, E. Niedermeyer and F. H. Lopes da Silva, Eds., 5th ed Philadelphia: Lippincott Williams & Wilkins, 2005, pp. 17-29.

[5] O. Creutzfeldt and J. Houchin, "Neuronal Basis of EEG-Waves (Section I)," in Handbook of Electroencephalography and Clinical Neurophysiology. vol. 2C, A. Remond, Ed., ed Amsterdam: Elsevier, 1974, pp. 5-55.

[6] B. Pesaran, "Uncovering the Mysterious Origins of Local Field Potentials," Neuron, vol. 61, pp. 1-2, 2009.

[7] A. J. Freeman, Mass action in the nervous system : examination of the neurophysiological basis of adaptive behavior through the EEG. New York: Academic Press, 1975.

[8] R. Pethig, "Ion, Electron, and Proton Transport in Membranes: A Review of the Physical Processes Involved," in Modern Bioelectrochemistry, F. Gutmann and H. Keyzer, Eds., ed New York: Plenum Press, 1986, pp. 199-239.

[9] B. Hille, Ion Channels of Excitable Membranes, Third ed. Sunderland, MA.: Sinauer Associates, Inc., 2001.

[10] C. Hales, et al., "Ion channel moment analysis reveals the endogenous local electric field dynamics of a biologically realistic spiking neuron," Journal of Neural Engineering, vol. tba, p. tba, 2011 Submitted.

[11] F. H. L. da Silva and A. Van Rotterdam, "Biophysical Aspects of EEG and Magnetoencephelogram Generation," in Electroencephalography : basic principles, clinical applications, and related fields, E. Niedermeyer and F. H. L. da Silva, Eds., 5th ed Philadelphia: Lippincott Williams & Wilkins, 2005, pp. xiii, 1309 p.

[12] P. Dayan and L. F. Abbott, Theoretical neuroscience : computational and mathematical modeling of neural systems. Cambridge, Mass. ; London: MIT Press, 2001.

[13] R. Ventura and K. M. Harris, "Three-dimensional relationships between hippocampal synapses and astrocytes," Journal of Neuroscience, vol. 19, pp. 6897-6906, Aug 1999.

[14] S. G. Hormuzdi, et al., "Electrical synapses: a dynamic signaling system that shapes the activity of neuronal networks," Biochimica Et Biophysica Acta-Biomembranes, vol. 1662, pp. 113-137, Mar 2004.

[15] D. Purves, Neuroscience, 3rd ed. Sunderland, Mass.: Sinauer Associates, 2004.

[16] L. P. Savtchenko and D. A. Rusakov, "The optimal height of the synaptic cleft," Proceedings of the National Academy of Sciences of the United States of America, vol. 104, pp. 1823-1828, Feb 2007.